

Determining the elastic modulus of biological samples using atomic force microscopy

Using the atomic force microscope (AFM) for nanoindentation has emerged as a useful tool to determine elastic properties like the elastic modulus for biological samples (figure 1) [1][2][3][4]. Cantilevers serve as soft nanoindenters allowing local testing of small and inhomogeneous samples like cells or tissues. To calculate the parameter of interest various models are used, but most of them are based on the Hertz model and extended to match the experimental conditions concerning the indenters' shape or the thickness of the sample [5][6][7][8][9][10][12].

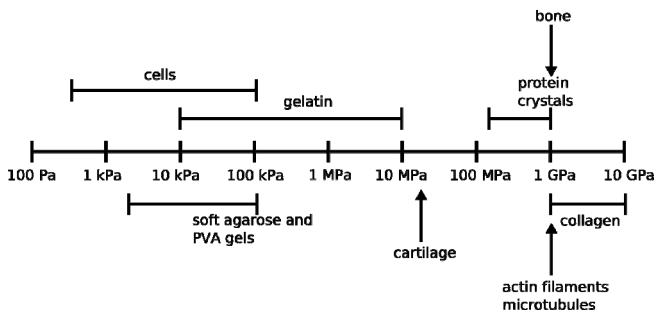


Fig. 1: Overview of the Young's modulus for different biological materials [5][8] [17][18][19].

Nanomechanical analysis of cells is becoming increasingly important in different fields like cancer and developmental biology. Differences in stiffness of normal and malign cells were found and also the change in metastatic potential with decreasing cellular stiffness can be marked [11][12][13][14]. Determining the cell cortex tension of zebrafish germ layer progenitors revealed differences in stiffness of the ecto-, meso- and endodermal progenitor cells [15]. Another example from the field of developmental biology is the mechanical testing of growth substrates. This application revealed the important role of matrix elasticity for cell lineage specification [16]. Not only cells but also components of their extracellular environment, like collagen fibrils have been tested for their mechanical properties [17]. The potential of this methodology is widely used in biological and also other disciplines to describe elastic properties of different matrices and materials [18][19][20].

This report describes the application and acquisition of elasticity experiments using AFM technique. An overview of the most commonly used model, the Hertz model is given and the assumptions and resulting limitations for the use with biological samples is discussed in detail.

The Hertz model

The Hertz model approximates the sample as an isotropic and linear elastic solid occupying an infinitely extending half space. Furthermore it is assumed that the indenter is not deformable and that there are no additional interactions between indenter and sample. If these conditions are met the Young's modulus (E) of the sample can be fitted or calculated using the Hertzian model. Several parameters describing the properties of the sample and indentation probe have to be specified.

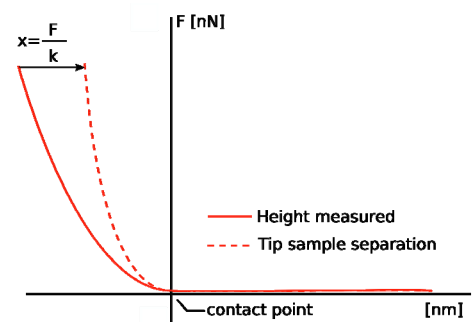
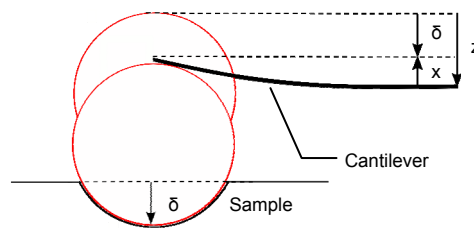


Fig. 2: Top - Sketch of the indentation experiment. The cantilever is moved towards the sample by a distance z (height (measured)). The cantilever is bending into the opposite direction (x) whilst the sample is indented by δ . Finally δ is calculated by subtracting the cantilever deflection from the height (measured). Bottom - Schematic of the correction of the height for the cantilever bending (x) to derive the tip-sample-separation (force indentation curve).

The data obtained by indentation measurements (force spectroscopy mode) are usually plots of force against piezo displacement, rather than tip sample separation. To apply the Hertz model, the curves need to be converted as explained in figure 2.

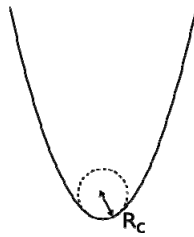
The parameter describing the sample is Poisson's ratio (ν) that depends on the material. For soft biological samples Poisson's ratio is generally set to 0.5 (incompressible materials like rubber). The geometry of the indenter then finally determines which equation is to be used. Different indenter geometries lead to different radii of the contact circle (a). The original Hertz model considers the shallow contact between two spherical bodies, but several extensions were made for different indenter geometries [9].

Parabolic

$$F = \frac{4\sqrt{R_c}}{3} \frac{E}{1-\nu^2} \delta^{3/2}$$

$$a = \sqrt{R_c \delta}$$

R_c = radius of tip curvature



Spherical

$$F = \frac{E}{1-\nu^2} \left[\frac{a^2 + R^2}{2} \ln \frac{R+a}{R-a} - aR \right]$$

$$\delta = \frac{a}{2} \ln \frac{R+a}{R-a}$$

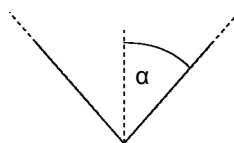
R = radius of the sphere

Conical

$$F = \frac{E}{1-\nu^2} \frac{2 \tan \alpha}{\pi} \delta^2$$

$$a = \frac{2 \tan \alpha}{\pi} \delta$$

α = semi-opening angle of the cone

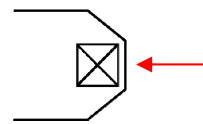


Four-sided pyramid

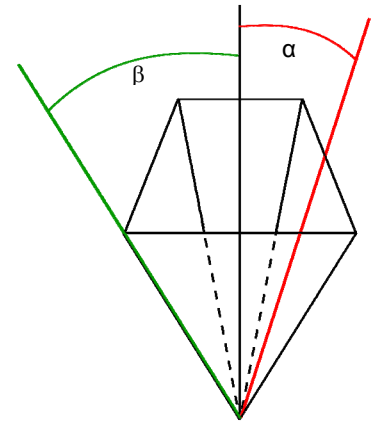
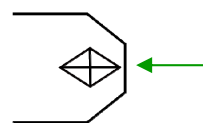
$$F = \frac{E}{1-\nu^2} \frac{\tan \alpha}{\sqrt{2}} \delta^2$$

$$a = \frac{\tan \alpha}{\sqrt{2}} \delta$$

α = face angle, usually given for Si_3N_4 -cantilevers



β = edge angle, usually given for Si-cantilevers



E can be derived using these equations by different methods. Usually it is calculated by fitting the force indentation curves (F - δ -curves) using E as a fit parameter. The contact point and baseline can also be used as variable fit parameters, or they can be determined before and used as a fixed value. Since it is very difficult to determine the real contact point (usually the curve has a very shallow angle around the contact point), so it is recommended to fit it.

The Hertz model assumes the indentation to be neglectable in comparison to the sample thickness, thus indentation depth has to be optimized. The Hertz model is valid for small indentations (say up to 5-10% of the height of the cell, maybe 200-500 nm) where the substrate does not influence the calculations. There may be additional limitations in indentation depth if the tip shape model is an approximation. Often the parabolic model is used if the indenter is a sphere because it is easier to fit and the approximation is reasonable for small indentations. The JPK IP software offers automatic fitting for all the indenter shapes shown here, so there is no longer any need to make this approximation.

Issues to be considered

The Hertz model makes several assumptions that are not truly met if cells or other biological samples are examined.

In this section these deviations are discussed and how to make the most reliable measurements.

Sample properties

The Hertz model assumes absolute elastic behavior as well as homogeneity of the sample. But most biological materials are neither homogeneous nor absolutely elastic. The energy delivered by the indenter is not completely given back by a cell (as it would be done by an absolute elastic material) but dissipates owing to plastic behavior that also appears as hysteresis between the extend and the retract part of the force curve (fig. 3). One time scale describing this behavior is the viscous relaxation time, which brings variations in force indentation measurements if different indentation velocities are tested [21][11]. Higher velocities result in a higher resistance of the sample material and the overall interaction is more viscous. Thus the higher the loading rate, the smaller is the indentation at a given force and the higher is the apparent stiffness. Indenting at time scales longer than the relaxation time will result in lower resistance of the sample and corresponding deeper indentations at a given force, because the cell material has time to move away from the indenting probe. However, at long time scales, the indentation stress can lead to irreversible reorganization of the cell. To reduce the influence of this time dependent behavior, an appropriate speed should be applied to prevent a too high viscous response or reorganization of the cell. It is of course crucial to stay consistent in velocity to have the same conditions for each experiment. Comparing different samples it should not be forgotten that each material or cell type has its own relaxation time since they can vary greatly in their composition (size of the nucleus, composition of the cytoplasm and cytoskeleton etc.).

Inhomogeneity of the sample also can result in artifacts like variation of the Young’s modulus depending on indentation depth, i.e. depending on the layer or component the indenter is actually pressing in. Cells have various components (like glycocalix, membrane extensions, nucleus, or organelles) that can reflect different stiffness. The contact point is also suffering from these variations and interactions of the probe and the sample surface or molecules that are covering the surface. Such curves often show a very shallow contact point where E is calculated to

be softer than the sample really is. The “real” stiffness of the sample thus only is measured when the probe reaches the proper surface that is after the shallow part of the curve. Then the fit doesn’t match the contact point of the Force-indentation-curve (figure 4). But this is not surprising since the Hertz model assumes homogeneity of the sample and no interactions between sample and probe. Finally, it is always important to focus on the part of the curve that represents the structure you want to investigate.

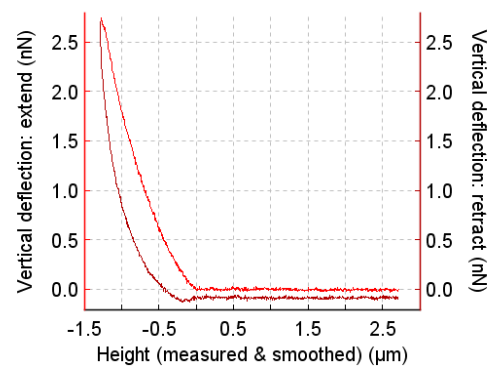


Fig. 3: Force distance curve taken on a living CHO cell (scan speed 5 μm/s). Trace (red) and retrace (dark red) curve clearly show hysteresis owing to the viscous and plastic behavior of the cell.

Fit range

Also important is to find the fit range that is to be used to yield optimum and reproducible results for elasticity calculations. As described in the section above E strongly fluctuates at very low indentations around the contact point but reaches a plateau with increasing indentation to finally increase again, mainly as a result of the substrate stiffness (glass slide etc., see figure 5, bottom). Thus the height of the indented structure is strongly to be considered. The Hertz model is only valid for small indentations (say up to 5-10% of the height of the cell, maybe 200-500 nm) where the substrate doesn’t influence the calculations and where the geometry of the indentation matches the geometry of the indenter. As described in the Hertz section above, the best way to find the optimum range is to record a force distance curve with relatively high indentation and to fit E for each point of the corresponding force indentation curve. Plotting E over indentation reveals the indentation when E

starts to tend towards a constant value that should be used to determine the Young's modulus (figure 5, middle).

But it can happen that there is no obvious plateau, especially when indenting inhomogeneous samples. If a cell for instance is tested right above the nucleus using a relatively small indenter (e.g. a pyramid), the nucleus can slip away from under the probe and the result is a decrease of the measured modulus right after the nucleus was pushed by the probe (figure 5, top).

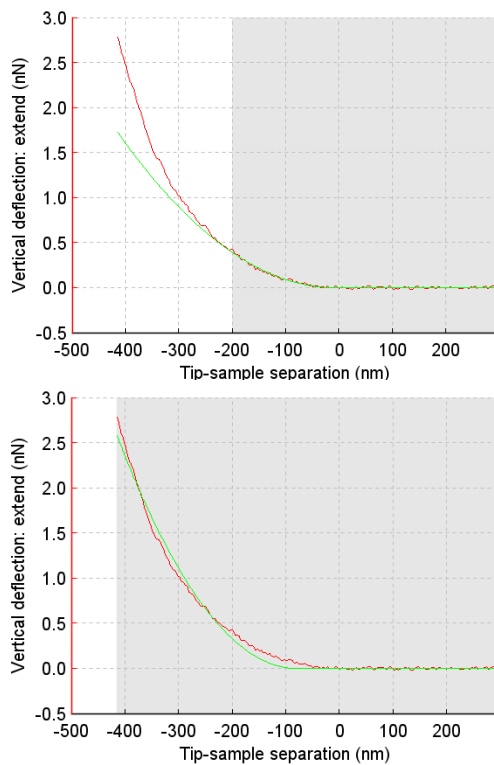


Fig. 4: Force versus indentation curves derived from a cell, fitted with the Hertz model. The same curve first was fitted to an indentation of 200 nm (top), and second over the whole indentation range of 400 nm (bottom). Obviously the probe pushed through two different layers since the fitted contact point of the first curve is different from the contact point of the second curve. The E module of the first curve, describing the stiffness of the cell surface, is about 16 kPa, the one of the second curve, that can be assumed to be the E module of the cytoplasm, about 35 kPa.

All three curves of figure 5 derive from the same cell and were taken with the same probe under exactly the same conditions. Even though there is no obvious “second”

increase in E and thus no obvious or typical hint of an effect of the glass substrate for both upper E versus indentation curves, the increase of the apparent stiffness from the cell centre to the edge indicates an influence of the substrate. But this is not surprising since the height of the cell at the nucleus was measured to be around 5 μm , at the surrounding of the nucleus to be around 1.3 μm and at the edge around 0.5 μm . Finally these results show that the effect of the substrate is not only visible by an increase of E within E versus indentation curves but also by increasing E values at thinner regions of the cells.

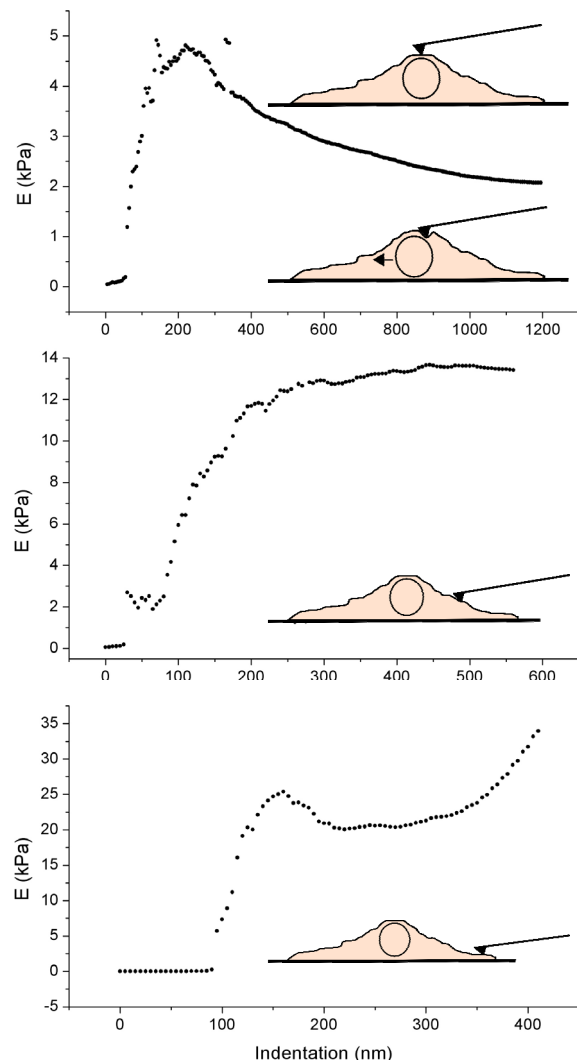


Fig. 5: E versus indentation curves of a CHO cell probed with a pyramidal indenter at different regions: right above the nucleus (top), the region next to the nucleus (middle) and near the edge

of the cell (bottom). Testing right above the nucleus (top) here only transiently denoted the stiffness of the nucleus. Obviously the nucleus was then pushed away resulting in decrease of E. Probing a relatively homogenous region (middle) revealed even indentation of the cytoplasm starting at around 250 nm. Indentation of the cell edge (bottom) leads to a second, substrate dependent increase of E starting at relatively low indentations.

Selection of the probe

Which cantilever should be used depends on the stiffness of the sample. As a rule of thumb one can keep in mind that the stiffness of the cantilever should be around the range of the sample stiffness. For cells that are very soft and delicate the softest cantilevers available with spring constants of around 10-30 mN/m should be used. For stiffer samples like agarose gels higher spring constants (30-100 mN/m or more) are appropriate.

Another point to consider is the choice of the indenter shape. For soft biological samples it is recommended to use spherical probes since the force is applied to a wider sample area than would be the case if a sharp pyramidal or conical tip is used, which results in a lower pressure. This way penetration of the sample is prevented. But this is not the only reason to prefer spherical indenters. Cells or tissues are very inhomogeneous, consisting of different components (nucleus, cytoskeletal components, organelles...). To yield a general impression for such inhomogeneous materials relatively big indenters like 20 μm beads are useful. To yield higher resolution, e.g. to test single cells or different cell parts, or to increase the pressure to indent stiffer materials beads of smaller diameters can be used (1-10 μm , depending on the desired resolution). Spheres are not always the best solution. If the sample is of very small dimensions or if different areas are to be tested in higher resolution (higher than one micron) pyramidal silicon nitride tips can be an alternative. A disadvantage of such more or less sharp tips is of course that they can penetrate the sample and thus lead to inaccurate calculations of the Young's modulus (generally a decrease of stiffness). But on the other hand they are less hindered by structures like cellular extensions or residues extending from the glycocalix than spheres are. Spherical indenters often feel such extensions, and the

result is a very shallow contact point that is extremely difficult to determine (which is also the reason why it should be fitted). A more general problem that occurs with cells is distorted force curves, mostly displayed as a "shoulder" in the contact region (fig. 6). These distortions can derive from contact with small structures like stress fibers or membranous extensions, which then slip away from the probe, leading to a second contact point.

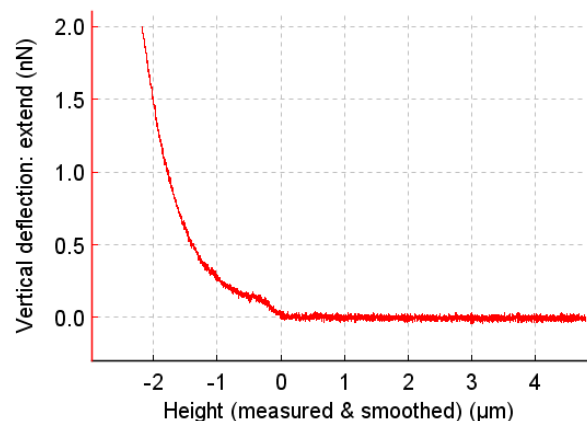


Fig. 6: Distorted extend curve taken on a CHO cell using a 2 μm spherical indenter.

Example of an indentation experiment

In this example the workflow to derive the Young's modulus of living CHO cells is described. The CellHesion[®] 200, mounted on a Zeiss optical microscope (AxioObserver), was used to prepare the spherical probe that was going to be used as well as to perform indentation experiments. The CellHesion[®] 200 is a new AFM based device, exclusively developed to meet the needs of testing cellular adhesion and mechanics. A PetriDishHeater[™] was used as a sample holder since cells were grown on WPI petri dishes. The cells were kept under physiological conditions during the whole experiment (37°C, HEPES buffered medium).

Preparation of the probe

Spherical indenters can either be purchased from special providers like particle probes from Novascan (0.6-25 μm glass spheres attached to cantilevers), or they can be homemade by gluing spheres on cantilevers. For such

purpose tipless cantilever are well suited. Care must be taken if cantilevers with tips are used, especially if small spheres are attached. This is because the sphere will attach to the side of the tip, rather than on the end, so that the tip will still have an impact on the experiment, especially if the chosen sphere diameter is less than the tip height. Silicon cantilevers have tips of up to around 15 μm . Thus tipless cantilevers would be better choice or at least silicon nitride cantilevers which have shorter tips (up to 5 μm).

For this example a tipless cantilever (Arrow TL1, NanoWorld, $k = 0.03 \text{ N/m}$) with an attached silica sphere (diameter 11 μm) was used as the indentation probe (fig. 7). The silica beads were attached to the cantilever with a two-part epoxy, but other biocompatible adhesives like optical adhesive are also well suited. This can easily be done by preparing a microscope slide where spheres are deposited on one part and epoxy on an adjacent part. If the beads are suspended in liquid, a drop is put on the slide and dried. A pair of clean tweezers can also be used to transfer dry beads onto the slide, or to spread the bead solution. Then a small amount of the epoxy is spread very thinly near the beads using a blade or pipette tip.

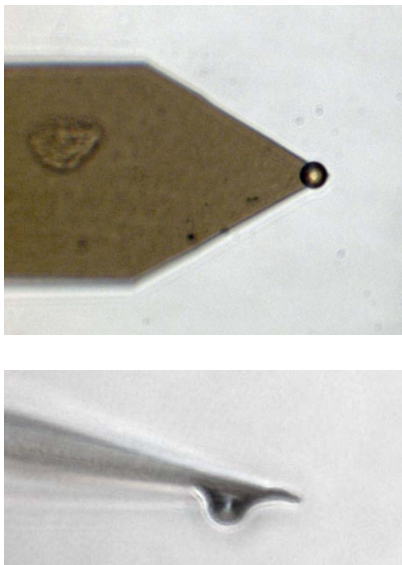


Fig. 7: Tipless cantilever with a 11 micron sphere attached

The cantilever must first be dipped into the epoxy. An approach is done on a clean region of glass to find the surface. Then the cantilever tip is positioned over the edge of the epoxy patch using the positioning screws and a force spectroscopy measurement is run to dip the tip into the glue. A setpoint of around 0.5 to 1 V should be sufficient. If there is too much glue on the tip it can flow over the bead and embed it. To prevent this, one or more additional spectroscopy measurements should be performed on a clean glass area. This will remove excess glue. Finally, to attach a sphere, another force curve is run with the tip positioned over a sphere.

Performing indentation experiments

The microsphere probe was mounted and aligned as usual on the AFM head. The WPI petri dish containing adherent CHO cells was mounted to the petri dish heater and the temperature was set to 37°C. The cantilever was then calibrated, i.e. the spring constant determined to be able to exactly specify the force to be applied to the sample. Using the NanoWizard® or CellHesion200® the calibration manager of the JPK SPM software leads the user through the calibration process, calculating the sensitivity by fitting a force curve (taken on a hard substrate) within the linear contact part and determining the spring constant with the thermal noise method. Once the calibration is complete, the desired setpoint force can be entered in Newtons (usually pico- or nano-Newtons). Now the experiment could be started.

Force distance curves were taken directly above the nucleus of different cells. Relatively high setpoints were used (up to 4 nN) since the mechanical properties of these cells were unknown. The extension/retract speed was set to 5 $\mu\text{m/s}$ and closed loop was used.

Data processing

The JPK DP software gives the possibility to derive the Young's modulus from force curves running through several steps (fig. 8). All operations have to be applied to the extend curve since it (normally or at least in fluid) contains no interactions like adhesion that make a determination of the contact point impossible. The first step of the processing is to remove any offset or tilt from the curve and find the contact point. Therefore the options

'Subtract baseline' and 'Find contact point' are to be selected. It is not essential to determine exactly the contact point or baseline offset here since they are variable fit parameters and don't have any influence on the fit results. Any tilt should be removed from the baseline since this is not part of the Hertz fit. The next step is to 'Correct height for cantilever bending', a feature that calculates the indentation depth by taking the difference between the piezo movement and the cantilever vertical deflection in units of length. Now the curves are ready to be fitted with the Hertz model to derive the Young's modulus. Other values, such as the fitted "contact point" and the fit quality parameter "residual RMS" are also displayed.

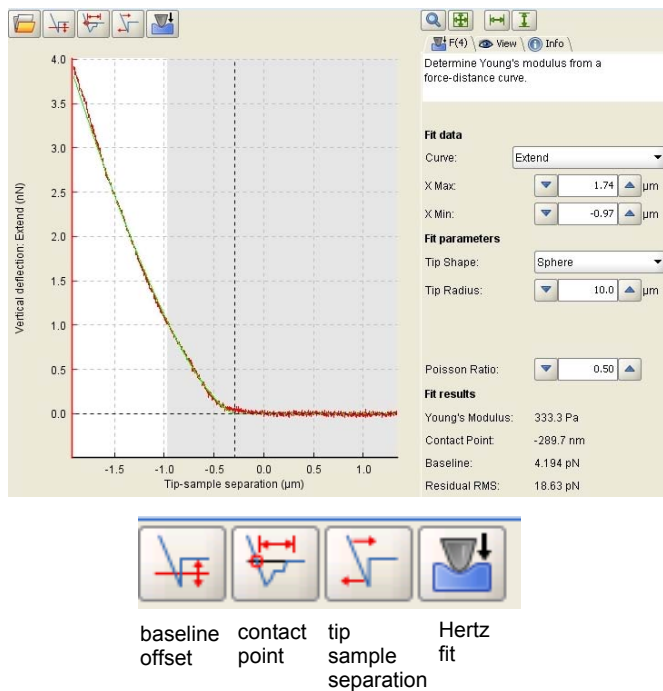


Fig. 8: Operations to derive the Young's modulus from a force curve. The first step is to remove any offset or tilt from the baseline and to find the contact point. In order to optimize the contact point determination the curve can be smoothed. The next and crucial step is to subtract the cantilever bending from the piezo movement to yield the indentation, i.e. a new channel called tip sample separation is created. Finally the Hertz model can be applied. The geometry of the indenter is to be specified as well as Poisson's ratio (that can be left at 0.5 for biological samples) and the data range to be fitted.

If many curves were recorded there is the possibility to use batch processing where all the described operations can be applied to a batch of curves (within one folder). Before batch processing, it is useful to examine a few curves in more detail to find the optimal fit range that can then be applied to all curves. Therefore the fit range should be increased stepwise till the E modulus tends towards a constant value. In figure 9 the Young's modulus derived from a CHO cell is plotted in dependence on indentation. Here E starts to take constant values at around 700-800 nm of indentation depth. If examining an array of curves, using batch processing, this value should be used for fit range. Of course the quality of the fit should always be checked by either looking directly at the curves or by comparing the residual RMS that is also written down in the results file that is generated when using batch processing.

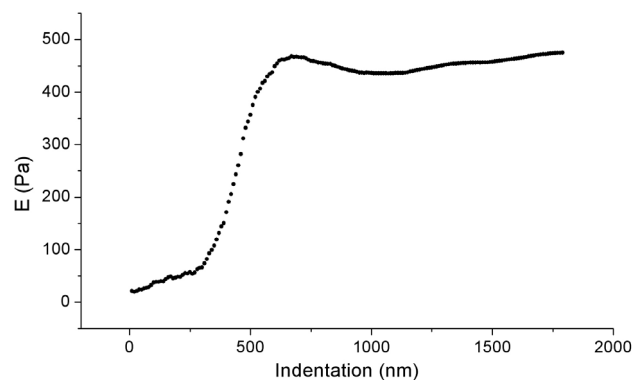


Fig. 9: E versus indentation curve of a CHO cell. At around 700 nm indentation E levels to a constant range (around 450 Pa).

Testing the system

The Young's modulus is often used to describe mechanical properties of cells and other samples. In many cases the intention to do such experiments is to compare the results with other data, produced by other researchers. Combing through the literature one always finds discrepancies between the E values of similar experiments but performed using different devices. To evaluate how the system works but also to gain a feeling for the technique and handling it is often useful to start with a sample where the elasticity has already been described with a similar system. Gels of polymers like agarose or polyvinyl alcohol are well-

described samples that are often used to describe principles of elasticity measurements [10][19][18].

To test the system on which the cell experiments were performed a 2.5% agarose gel was indented using a 11 μm spherical probe. Since agarose gels in this concentration are stiffer than cells, stiffer probes have to be used, e.g. with spring constants of 0.5-5 N/m. In this example a NSC cantilever from mikromasch (4 N/m) was used. The corresponding E versus indentation curve is shown in figure 10 displaying a final E of around 36 kPa. This value agrees well with the literature (figure 1, [19]).

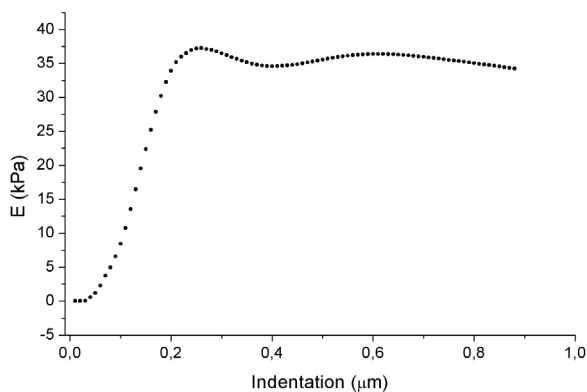


Fig. 10: E versus indentation curve calculated for a force distance curve taken on a 2,5% agarose gel using a 11 μm spherical probe with a spring constant of 4 N/m. The final E is around 36 kPa

Conclusion

In spite of some limitations the Hertz model is a helpful and commonly used method to express mechanical properties of biological samples like cells. There are some issues that should be kept in mind such as the fit range or composition of the sample. Biological samples often display viscoelastic behavior and they are inhomogeneous, i.e. consist of different “materials” with different elastic properties. To know exactly which component exactly is described by the results it is most important to become acquainted with the sample and to adequately adjust the parameters. Considering all these issues will help to yield reasonable and reproducible results.

The JPK NanoWizard[®] or the CellHesion[®] in combination with dedicated sample holders, like the PetriDishHeater[™] or the BioCell[™], provide the means to obtain elasticity data (among numerous other data types) for biological samples. Additionally the JPK DP software helps the user through all steps to prepare the acquired curves for Hertz processing and provides an easy to use calculator for the Young’s modulus.

Literature

- [1] Kunda P., Pelling A.E., Liu T., Baum B.: Moesin controls cortical rigidity, cell rounding, and spindle morphogenesis during mitosis, *Current Biology* 18:91-101, January 2008
- [2] Ludwig T., Kirmse R., Poole K., Schwarz U.S.: Probing cellular microenvironments and tissue remodeling by atomic force microscopy, *Pflugers Archiv: European Journal of Physiology* 456:29-49, April 2008
- [3] Lu Y.-B., Franze K., Seifert G., Steinhäuser C., Kirchhoff F., Wolburg H., Guck J., Janmey P., Wei E.-Q., Käs J., Reichenbach A.: Viscoelastic properties of individual glial cells and neurons in the CNS, *PNAS* 103:17759-17764, November 2006
- [4] Brunner C.A., Ehrlicher A., Kohlstrunk B., Knebel D., Käs J.A., Goegler M.: Cell migration through small gaps, *European Biophysical Journal* 35:713-719, June 2006
- [5] Alonso J.L., Goldmann W.H.: Feeling the forces: Atomic force microscopy in cell biology, *Life Sciences* 72:2553-2560, 2003
- [6] Hertz H.: Über die Berührung fester elastischer Körper, *Journal für die reine und angewandte Mathematik* 92:156-171, 1881
- [7] Sneddon I.N.: The relation between load and penetration in the axisymmetric Boussinesq problem for a punch of arbitrary profile, *International Journal of Engineering Science* 3:47-57, May 1965
- [8] Casademunt J.A.: Micromechanics of cultured human bronchial epithelial cells measured with atomic force microscopy, PhD thesis, Universitat de Barcelona, 2001
- [9] Lin D.C., Dimitridas E.K., Horkay F.: Robust strategies for automated AFM force curve analysis-I. Non-adhesive indentation of soft, inhomogeneous materials, *ASME* 129:430-440, June 2007
- [10] Rico F., Roca-Cusachs P., Gavara N., Farré R., Rotger M., Navajas D.: Probing mechanical properties of living cells by atomic force microscopy with blunted pyramidal cantilever tips, *Physical Review* 72:021914, August 2005

- [11] Rosenbluth M.J., Lam W.A., Fletcher D.A.: Force microscopy of nonadherent cells: A comparison of leukemia cell deformability, *BiophysJ* 90:2994-3003, April 2006
- [12] Docheva D. Padula D., Popov C., Mutschler W., Clausen-Schaumann H., Schieker M., Researching into the cellular shape, volume and elasticity of mesenchymal stem cells, osteoblasts and osteosarcoma cells by atomic force microscopy, *Journal of Cellular and Molecular Medicine* 12:537-552, October 2007
- [13] Cross S.E., Jin Y.-S., Rao J., Gimzewski J.K.: Nanomechanical analysis of cells from cancer patients, *Nature Nanotechnology* 2:780-783, December 2007
- [14] Darling E.M., Zauscher S., Block J.A., Guilak F., A thin-layer model for viscoelastic, stress-relaxation testing of cells using atomic force microscopy: do cell properties reflect metastatic potential?, *Biophysical Journal* 92:1784-1791, March 2007
- [15] Krieg M., Arboleda-Estudillo Y., Puech P.-H., Käfer J., Graner F., Müller D.J., Heisenberg C.-P.: Tensile forces govern germ-layer organization in zebrafish, *Nature Cell Biology* 10:429-436, April 2008
- [16] Engler A.J., Sen S., Sweeney H.L., Discher D.E.: Matrix elasticity directs stem cell lineage specification, *Cell* 126:677-689, August 2006
- [17] Wenger M.P.E., Bozec L., Horton M.A., Mesquida P.: Mechanical properties of collagen fibrils, *Biophysical Journal* 93:1255-1263, August 2007
- [18] Dimitriadis EK., Horkay F., Maresca J., Kachar B., Chadwick RS.: Determination of Elastic Moduli of Thin Layers of Soft Materials Using the Atomic Force Microscope, *Biophysical Journal* 82:2789-2810, May 2002
- [19] Stolz M., Raiteri R., Daniels AU., VanLandingham MR., Baschong W., Aebi U.: Dynamic Elastic Modulus of Porcine Articular Cartilage Determined at Two Different Levels of Tissue Organization by Indentation-Type Atomic Force Microscopy, *Biophysical Journal* 86:3269-3283, May 2004
- [20] Touhami A., Nysten B., Dufrêne YF.: Nanoscale Mapping of the Elasticity of Microbial Cells by Atomic Force Microscopy, *Langmuir* 19:4539-4543, March 2003
- [21] Li Q.S., Lee G.Y.H., Ong C.N., Lim C.T.: AFM indentation study of breast cancer cells, *BiochemBiophysResCom* 374:609-613, July 2008